Characterization of neointima lesions associated with arteriovenous fistulas in a mouse model

Y Castier[1], S Lehoux[1], Y Hu[2], G Fonteinos[2], A Tedgui[1] and Q Xu[2]

[1]INSERM Centre de Recherche Cardiovasculaire Lariboisiere, Paris, France and [2]Department of Cardiac and Vascular Sciences, St George's University of London, London, UK

Arteriovenous fistulas (AVFs) are usually used for vascular access in the provision of hemodialysis, but AVFs have a 1-year patency rate of only about 60% owing to stenosis. As the molecular mechanisms behind AVF neointimal hyperplasia remain largely unknown, representative models in transgenic mice could be useful to study this process at the genetic level. Hence, we characterized neointimal lesion formation in a model of AVF recently developed in the mouse, where the common carotid artery was end-to-side sutured to jugular vein in C57BL/6J mice. At the site of anastomosis, arterial wall thickening was observed as early as 1 week after surgery (fourfold) and progressed to six- and 10-fold original thickness in carotid arteries after 2 and 3 weeks, respectively. The lumen of the carotid artery was significantly narrowed owing to neointima hyperplasia, and thrombosis was observed in the vein wall opposite to the anastomosed artery. Histological and immunohistochemical analyses revealed that 3-week neointimal lesions consisted of abundant smooth muscle cells (alpha-actin$^+$) and a small number of membrane attack complex-1+ macrophages. Furthermore, using chimeric mice receiving bone marrow from transgenic mice expressing the LacZ gene in smooth muscle (SM-LacZ), it was found that bone marrow stem cells did not contribute to smooth muscle cell accumulation in neointimal lesions of AVF arteries. Thus, this model, which reproduces many of the features of human AVF, should prove useful for our understanding of the mechanism of neointimal formation and to evaluate the effects of drugs and gene therapy on this disease.

Correspondence: Q Xu, Department of Cardiac and Vascular Sciences, St George's University of London, Cranmer Terrace, London SW17 0RE, UK. E-mail: q.xu@sghms.ac.uk

Hemodialysis vascular access dysfunction is one of the most important causes for morbidity in hemodialysis patients, who are approximately a quarter million and growing at the rate of 5% per annum in the US.[1] Concomitantly, it has been estimated that vascular access dysfunction is responsible for more than 20% of all hospitalizations in the end-stage renal disease population.[2] The native arteriovenous fistula (AVF) is frequently used for vascular access in the provision of hemodialysis. Unfortunately, AVFs have a 1-year patency rate of only about 60% and a 2-year patency of about 40%. The major cause for AVF failure is neointimal hyperplasia leading to the development of stenosis and subsequent thrombosis, but the mechanisms of this neointimal formation remains poorly understood.[3,4]

Peripheral AVFs have been described in small animal such as rats and rabbits at the femoral or carotid levels.[5,6] The ability to introduce transgenes or to disrupt endogenous gene expression has made the mouse an attractive species for this model. However, the most widely used AVF in mice is an aortocaval shunt, which predisposes to major hemodynamic modifications leading to cardiac failure.[7,8] The use of a more peripheral AVF in mice to reproduce native AVF for hemodialysis in humans has not been described, to the best of our knowledge.

Many studies have suggested that progenitor cells can participate in the pathogenesis of vascular diseases in models of allograft vasculopathy, postangioplasty restenosis, and hyperlipidemia-induced atherosclerosis contributing to smooth muscle cell (SMC) accumulation.[9–16] On the other hand, other reports have cast doubt on the pluripotential of adult stem cells *in vivo* under physiological conditions.[17] Similarly, it was reported that bone marrow stem cells might not contribute to the formation of mature SMCs in allograft-induced neointimal lesions.[15] It is unknown whether progenitor cells play a role in the neointima formation either in humans or in animal models of AVF.

The purposes of the present study were to characterize the neointima lesions that evolve after the creation of an AVF in mice and to investigate the potential role of progenitor cells in the neointima formation in this model.

RESULTS
Neointimal formation in the artery and vein
AVF was performed in the mouse via end-to-side anastomosis of the carotid artery and jugular vein, as illustrated by a schematic picture and actual photograph in Figure 1a and d, respectively. The overall perioperative mortality was 20% and deaths were mainly related to either anesthesia or hemorrhage during recovery. All the AVFs analyzed in this study were patent at the time of harvesting up to 3 weeks (vessel patency at 3 weeks: 100%). The lumen of some AVFs started to be occluded after 3 weeks and only one-third of vessels were patent 4 weeks after surgery. Detailed hemodynamic analyses are reported elsewhere.[18] Briefly, blood flow was increased more than six-fold in the RCCA proximal to the AVF, but systemic blood pressure and heart rate remained unchanged.[18]

We made a series of sections along the carotid artery. Figure 2 shows the development of neointimal lesions 3 weeks after creation of the fistula at the different levels near the anastomosis. At the proximal end of the artery, a normal vessel structure, that is, 2–3 layers of cells in the vessel wall (Figure 2a) was observed, associated with an increase in vessel caliber in response to enhanced flow (see detailed description in Castier *et al.*[18]). Neointimal lesions were observed in the artery near the site of anastomosis (Figure 2b and c), and maximal lesion formation was found at the level around the suture (Figure 2d). A proportion of the lesions protruded into the lumen of the jugular vein beyond the suture (Figure 2e).

Furthermore, the jugular vein of control animals had a thin vessel wall (two or three cellular layers) surrounded by perivascular tissue (Figure 2f), whereas the venous wall opposite to the anastomosis revealed an increased thickness 3 weeks after AVF was established (Figure 2g and h). Neointimal hyperplasia ranged from modest thickening of the venous wall associated with a small thrombus (Figure 2g) to more predominant hyperplasia extending in a papilliform into a much larger thrombus (Figure 2h). Heterogeneity of venous lesions was observed opposite to the anastomosis. The initiation, development, and distribution of lesions in the model are schematically represented in Figure 1b and c.
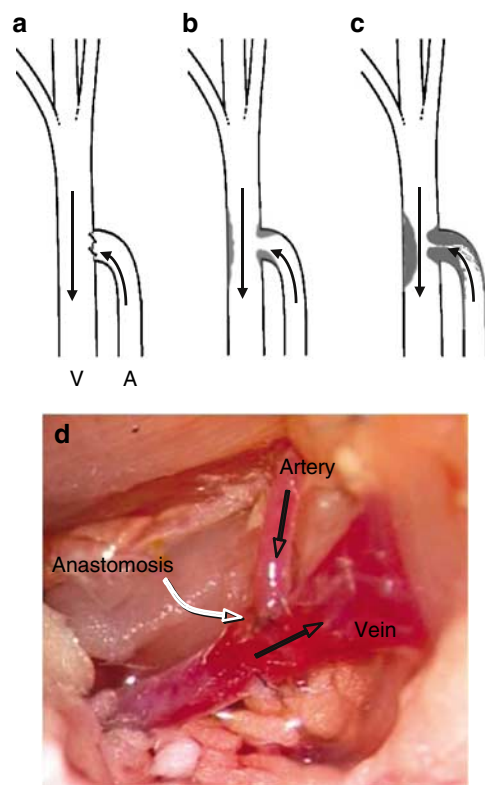

Figure 1 | Schematic representation of AVF-associated lesion formation in mice. A window was cut on the side of the jugular vein, and the carotid artery was transected distally and sutured to the vein. (**a**) Arrows represent direction of blood flow in the artery (A) and vein (V). (**b**) Lesion formation (gray shading) occurred at the site of anastomosis and on the vein wall opposite to the arterial opening. (**c**) Lesion size progressed with time, encroaching on the lumen, and protruding into the vein. Panel (**d**) shows a photograph of an AVF after performing anastomosis, with black arrows indicating the direction of blood flow. Note that the head of the mouse is at the left and the heart at the right.
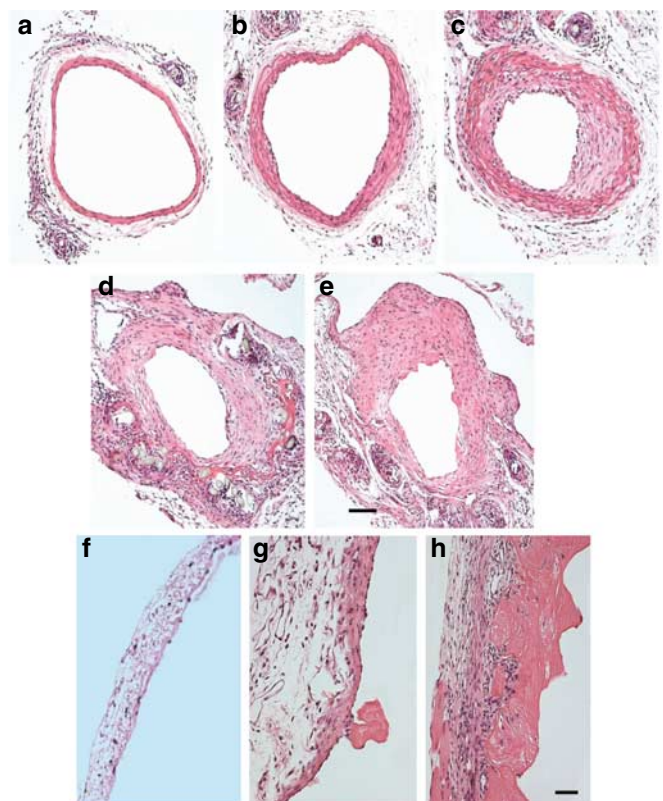

Figure 2 | Hematoxylin and eosin-stained sections of mouse artery and vein at the site of AVF anastomosis. At 3 weeks after opening of the AVF, vascular segments were fixed *in situ* in 4% phosphate-buffered formaldehyde (pH 7.2), embedded in paraffin, sectioned, and stained with hematoxylin–eosin. A series of sections were cut in the artery at different levels approaching (**a**–**e**) the anastomosis and (**f**–**h**) in the vein. Note that the lesion size increases near (**d**) the anastomosis. (**f**) Shows a normal vein vessel wall before surgery, whereas (**g** and **h**) represent vein sections 3 weeks after AVF. Bar $= 50 \mu$m.

Figure 3 shows representative cross-sections with neointima hyperplasia progressing throughout the four time points. Neointimal lesions were observed in the artery near the suture at 1 week, and became larger at 2 and 3 weeks (Figure 3b, c and d). Figure 3e–h are representative photographs at higher magnification corresponding to Figure 3a–d. Histomorphometric analysis showed that neointimal lesions were strongly correlated with the time of fistula establishment ($P = 6.95 \times 10^{-6}$). Lesion area (μm^2) measured at the site of the suture increased from $37\,272 \pm 3520$ at 1 week to $105\,519 \pm 8676$ at 3 weeks. In parallel, the lumen size of the carotid artery reduced progressively with time after AVF creation, such that 3 weeks after surgery the lumen was almost closed by neointimal lesions (Figure 3 lower panel). To verify whether the suture material could be at cause, arterial remodeling was investigated in a group of sham animals having a suture tied around the right carotid artery during 4 weeks. We found no change in artery thickness and no inflammatory cell infiltration in such arteries (data not shown).
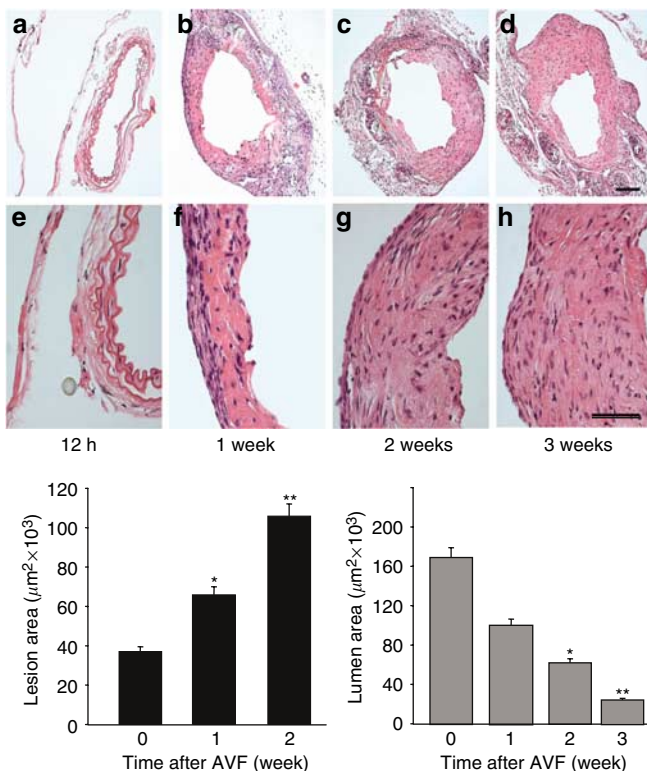
Cell composition

To study cell composition of neointimal lesions, sections were probed with antibodies against macrophages, T cells, and SMCs. Membrane attack complex-1 (MAC-1) + monocytes/macrophages were observed as early as 1 week after operation (Figure 4b), whereas negative controls stained with normal rat immunoglobulin (Figure 4a) displayed no positive staining. The results shown in Figure 4c indicate abundant macrophages in 2-week neointimal lesions, whereas fewer MAC-1 + cells were present in the lesion 3 weeks after creation of the AVF (Figure 4d). These cells were also frequently found in the adventitia at all three time points, particularly around the suture areas. T lymphocytes were rarely found in the neointima, and were absent from the adventitia (data not shown).

α-Actin is widely used as a marker of vascular SMCs, although not all SMCs positively stain with antibody against α-actin. Furthermore, immunoreactivity for α-actin is reduced in rapidly replicating SMCs.[19] Similar to findings reported previously, we observed a very weak staining for α-actin, if any, at 1 and 2 weeks after creation of the AVF (Figure 4e and g). Nonspecific staining in negative controls (Figure 4e) was minimal. Figure 4h demonstrates the presence of abundant SMCs in the mature neointimal lesion observed 3 weeks after creation of the AVF, indicating that SMC accumulation at the site of anastomosis played an
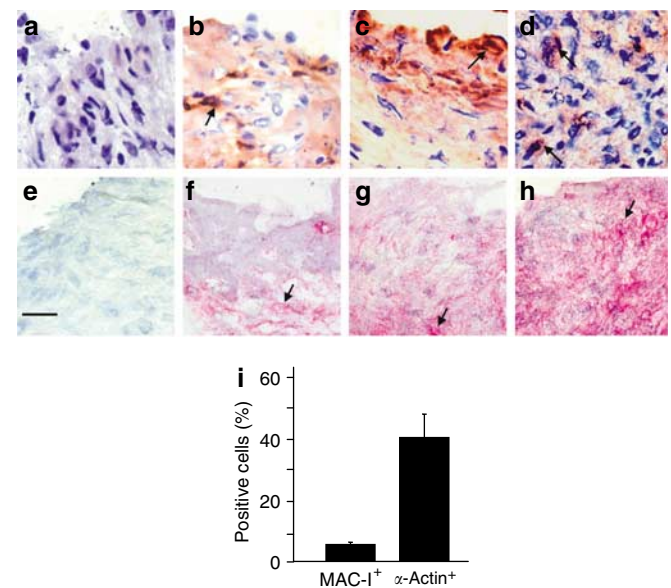

12 h 1 week 2 weeks 3 weeks

Figure 3 | Neointimal quantification in the AVF anastomosis. Hematoxylin and eosin-stained sections were prepared as described in Figure 2. Lesion area was measured microscopically as described in the Materials and Methods. (a–d) Representative pictures of anastomoses obtained 12 h, 1 week, 2 weeks, and 3 weeks after AVF creation. Panels (e–h) are photographs at higher magnification corresponding to panels (a–d). Bar = 50 μm. The graph shows mean ± s.d. ($n = 6$/group). *$P < 0.05$ and **$P < 0.01$ versus unoperated controls.

Figure 4 | Immunohistochemical staining demonstrates the presence of MAC-1 + mononuclear cells and SMCs in neointimal lesions 3 weeks post-AVF. Frozen sections derived from the site of anastomosis in arteries at (a and b) 1, (c) 2, and (d) 3 weeks post-AVF were probed with normal rat immunoglobulin or with a rat monoclonal antibody (CD11b/18; b–d) against MAC-1 + leukocytes. For SMC staining, sections of arteries obtained (e and f) 1, (g) 2, and 3 weeks post-AVF were probed with (e) normal mouse serum or with (f–h) a mouse monoclonal anti-α-actin antibody. A counterstaining (blue) with hematoxylin was performed. Arrows indicate typical positive cells. Bar = 10 μm. The graph shows mean ± s.d. ($n = 6$/group) (i).

important role in neointimal lesion formation in this model. Data summarized in Figure 4i indicates that a large proportion of neointimal cells were SMCs, although MAC-1+ cells were also present.

Cell origins in neointimal lesions

To determine the source of neointimal SMCs, chimeric mice were used for AVF construction. We performed experiments with C57/BL6J chimeric mice which had received SM-LacZ[20] bone marrow cells after irradiation. When AVFs were established in these irradiated mice (C57/BL6J/SM-LacZ BM), which had only β-gal activity in bone marrow cells or marrow-derived cells, no β-gal-positive cells were observed in the neointimal lesions (Figure 5c). We also performed double staining for α-actin and β-gal in sections of the neointimal lesions from C57/BL6J/SM-LacZ BM chimeric mice with bone marrow β-gal positivity. Data shown in Figure 5d indicates the absence of double positive cells, although many cells showed α-actin+. As expected, β-gal+ cells were observed in the arterial wall of the SM-LacZ mouse (Figure 5a), whereas vessels derived from C57/BL6J mice were β-gal negative (Figure 5b). These findings indicate that neointimal cells were not derived from bone marrow cells.

DISCUSSION

In the present report, we have characterized a new model of neointimal hyperplasia in the mouse that occurs at the site of anastomosis connecting the carotid artery and the jugular vein. This neointimal hyperplasia develops mainly around the anastomosis and shows a rapid accumulation of SMCs. Furthermore, we provide strong evidence that bone marrow cells do not contribute to the deposition of SMCs in the
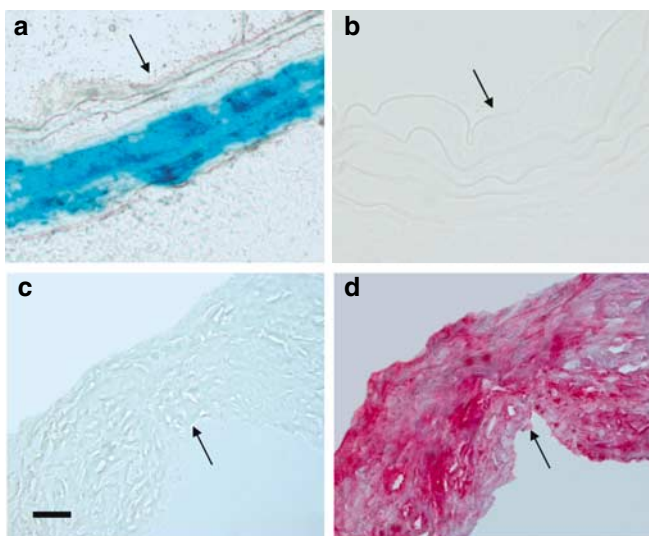

Figure 5 | Non-bone marrow origin of SMCs in neointimal lesions. Bone marrow cells of SM-LacZ mice were transplanted into irradiated wild-type mice 3 weeks before AVF surgery. Frozen sections were stained for (a–c) X-gal or for both X-gal and (d) α-actin. (a and b) Carotid arteries from SM-LacZ and wild-type mice, respectively. (c and d) Sections from AVF artery anatomoses. Arrows indicate the luminal surface of the vessels. Bar = 50 μm.

development of neointimal lesions in our model. To our knowledge, this is the first time that a mouse model of neointima hyperplasia in response to a 'peripheral' AVF has been established. We believe that this model could be useful for studying the pathogenesis of AVF-induced neointimal formation, because the well-defined genetic systems of mice make this species an attractive experimental model for vascular biology research.[21]

The AVF is the vascular access of choice in the provision of hemodialysis, and dysfunction and failure of AVFs necessitate less desirable vascular accesses such as polytetrafluoroethylene grafts and central venous catheters. Vascular access-related morbidity severely impairs the welfare of patients with end-stage renal disease and greatly amplifies the cost of their medical care.[1,2] In patients, the occurrence of uremia may influence the neointmal formation in AVF. Although the mice we used were not uremic, we suggest that our model may be used to explore mechanisms of neointima formation that contribute to the dysfunction and failure of AVFs used for vascular access in patients with end-stage renal disease.

The mouse model of central (aortocaval) AVF incurs major hemodynamic modifications leading to cardiac failure.[7,8] In this respect, our model of a more peripheral AVF at the cervical level is particularly valuable as it does not modify the arterial blood pressure. Another chief advantage of the murine model is the short period necessary (3 weeks) to develop significant neointimal lesions, thereby facilitating relatively short-term intervention or genetics studies. Moreover, to perform the AVF, we mimicked the suturing technique which is used for constructing AVFs in clinical practice. Although our model is technically demanding, with experience we were able to achieve a surgical success rate (fistula patent at 3 weeks) of about 90%.

We show that neointimal hyperplasia develops rapidly in our model and is mainly located around the anastomosis, the site most relevant to clinical states. In this AVF model, flow rate increased sevenfold in the artery upstream of the anastomosis, producing a marked artery enlargement as previously reported.[18] Although increased flow is known to inhibit neointimal hyperplasia,[22,23] altered biomechanical stress at the site of anastomosis may have stimulated SMCs to proliferate and accumulate in the intima.[24] The turbulent blood flow near the anastomosis, the surgical traumatism, and the compliance mismatch between artery and vein are believed to be factors that may have engendered this juxta-anastomotic lesion.

The source of SMCs in neointimal lesions is a fundamental issue in understanding the pathogenetic interactions of cells involved in the disease process. Recent reports demonstrated that progenitor cells are present in the adventitia[25] and that bone marrow cells may contribute to the accumulation of SMCs within neointimal lesions.[11–13] In the present report, we provide evidence that neointimal SMCs of AVF anastomoses do not originate from bone marrow stem cells, as identified directly by SMC SM22-driven β-gal expression. Rather, we demonstrate a weak

staining for α-actin in the early lesions, which progresses with time and becomes strong in advanced lesions, suggesting a maturation process of SMCs. However, we cannot exclude the contribution of stem cells, for example, adventitial and circulating SMC progenitors, to SMC accumulation in the neointimal lesions of arteries with AVFs.

In summary, we have characterized a new mouse model for AVF that shares some similarities with human AVFs. The lesions consist mainly of SMCs which do not appear to be derived from bone marrow stem cells. We believe that this model could be useful for studying the pathogenesis of neointimal formation for AVF-induced stenosis.

MATERIALS AND METHODS
Mice
All animal experiments were performed according to protocols approved by the Institutional Committee for Use and Care of Laboratory Animals. C57BL/6J mice were purchased from the Charles River Laboratory (Les Oncins, France). Transgenic SM-LacZ mice expressing β-gal under the control of the smooth muscle-specific protein SM22 promoter have been described previously.[26,27] The mice were maintained on a light/dark (12/12 h) cycle at 22°C receiving food and water *ad libitum*. The genetic constitution of all mice used in the present study was C57BL/6.

Creation of arteriovenous fistula
AVFs were created in mice as recently described.[18] Mice were anesthetized by intraperitoneal injection of a mixture of ketamine hydrochloride (0.20 mg/g) and xylazine (0.02 mg/g). After adequate shaving and preparation of the neck skin, the mice were fixed in a supine position with its neck extended. Each animal received 1 IU/g of heparin at the onset of the procedure. The operation was performed under a dissecting microscope (Nikon SMZ 1000). Through a midline skin incision of the neck, the right common carotid artery (RCCA) and external jugular vein (JV) were dissected and exposed. The right cleidomastoid muscle was resected. All branches of the JV were ligated (ethilon 10-0, Ethicon, Issy-Les-Moulineau). The RCCA was clamped proximally, ligated just below the carotid bifurcation with an 8-0 ethilon and transected. The JV was clamped proximally and distally and a small venotomy was performed in its middle part. Using microsurgical sutures (ethilon 11-0, Ethicon), an end-to-side RCCA/JV anastomosis was completed with six interrupted sutures. Thereafter, the vascular clamps were removed and fistula patency was verified. The operative field and the vessel lumen were irrigated with a saline solution containing 100 IU/ml of heparin. The skin was then closed with continuous stitches using 6-0 vicryl. Operative time averaged 80 min, animals were kept warm until complete recovery under a heating lamp, and 1.5 ml of saline solution was injected subcutaneously at the end of the procedure. The carotid–jugular fistula is schematically illustrated in Figure 1a.

Tissue harvesting
At the time of killing, all the animals in this study were first anesthetized and the fistula was dissected to assess its patency. Thereafter, animals were killed by overdose of sodium pentobarbital and tissues harvested for different analyses. For histological analysis, mice were perfused briefly (1 min) at 80 mm Hg with 0.9% NaCl solution via an abdominal aortic cannulation, and subsequently perfusion fixed with 4% phosphate-buffered formaldehyde (pH 7.2) for 15 min. To determine the time course of neointima formation, we harvested the JV and RCCA adjacent to the anastomosis at postoperative weeks 1, 2, and 3 (six animals per group). Samples were fixed with 4% phosphate-buffered formaldehyde at 4°C for at least 24 h. For frozen section preparation, AVFs were harvested, immediately frozen in liquid nitrogen, and stored at −80°C.

Bone marrow transplantation
The procedure used for creating chimeric mice was similar to that described previously.[25,28] Briefly, donor mice were killed and the femurs and tibias were removed aseptically. Marrow cavities were flushed with Ca,Mg-free Hanks' balanced salt solution (GIBCO-BRL, Paisley) using a 25-gauge needle attached to a syringe. Single cell suspensions were prepared by repeat pipetting, and the cell preparations passed through a 120 μm nylon mesh filter to remove particulate matter. Cells were washed twice in Hanks' balanced salt solution, counted using a hemocytometer, and resuspended at 3×10^7 cells/ml before transplantation. Six- to eight-week-old mice received a lethal dose of whole body X-ray irradiation (950 Rads) as described previously.[15] The irradiated recipients received 1×10^7 bone marrow cells in 0.3 ml RPMI 1640 by tail vein injection. Six animals were included for each group.

Histology and lesion quantification
After fixation, the samples were dehydrated in graded ethanol baths, cleared in xylol, and embedded in paraffin.[29] Histological sectioning began at the arterial segment 1 mm above the anastomosis. Routinely, 7 μm-thick sections were made throughout the dissected fragments, stained with hematoxylin and eosin, and examined microscopically (Zeiss, Göttingen, Germany). The procedure for lesion area measurement is similar to that described elsewhere.[30] Using a transmission scanning microscope (LSM 510, Zeiss), vessels were scanned, saved, and the lumen and perilesional tissue were outlined using image analysis software. The lesion area was determined by subtracting the area of the lumen from the area enclosed by the internal elastic lamina. Lesion areas were measured and recorded in square micrometers. When making vessel sections, all sections were placed on slides and verified using a microscope. The cross-section with greatest lesion size and six supplemental cross-sections (three upstream, three downstream) situated at 28 μm intervals were chosen for analysis.

Immunohistochemical staining
Serial 7 μm-thick frozen sections were cut from cryopreserved tissue blocks and the procedure used in the present study for immuno-histochemical staining was similar to that described previously.[25,28] Briefly, macrophages were identified by application of a rat monoclonal antibody (CD11b/18) against mouse MAC-1 leukocytes (Pharmingen, San Jose, CA, USA) followed by biotinylated anti-rat immunoglobulin secondary antibody (Dako-Glostrup, Denmark). Smooth muscle cells were identified with a mouse monoclonal antibody against α-actin labeled with phosphatase (Sigma, St Louis, MO, USA) followed by Fast Red Tr/Naphthol AS-MX (Sigma). The surface of positive-stained cells in the lesion was counted and expressed as the percentage of total area.

β-Gal staining and double fluorescence labeling
The procedure for determining β-gal activity in sections was similar to that described by Sanes *et al.*[31] Briefly, sections were incubated at

37°C for 18 h in PBS supplemented with 1 mg/ml X-Gal (Sigma).[32] For double staining of β-gal and SMC α-actin, we performed SMC α-actin staining before β-gal staining. SMCs were identified with a mouse monoclonal antibody against α-actin conjugated with phosphotase (Sigma).

Statistical analysis

Statistical analyses were performed on a Macintosh computer with StatView software using the Mann–Whitney U-test and analysis of variance. Results are expressed as mean $\pm$ s.d. A P-value < 0.05 was considered significant.

REFERENCES

1. United-States Renal Data Systems. SRDS 2004 annual data report. *Am J Kidney Dis* 2005; **45**: 8–280.
2. Rayner HC, Pisoni RL, Bommer J *et al.* Mortality and hospitalization in haemodialysis patients in five European countries: results from the Dialysis Outcomes and Practice Patterns Study (DOPPS). *Nephrol Dial Transplant* 2004; **19**: 108–120.
3. Roy-Chaudhury P, Kelly BS, Zhang J *et al.* Hemodialysis vascular access dysfunction: from pathophysiology to novel therapies. *Blood Purif* 2003; **21**: 99–110.
4. Rotmans JI, Pasterkamp G, Verhagen HJ *et al.* Hemodialysis access graft failure: time to revisit an unmet clinical need? *J Nephrol* 2005; **18**: 9–20.
5. Tronc F, Mallat Z, Lehoux S *et al.* Role of matrix metalloproteinases in blood flow-induced arterial enlargement: interaction with NO. *Arterioscler Thromb Vasc Biol* 2000; **20**: E120–E126.
6. Qin F, Dardik H, Pangilinan A *et al.* Remodeling and suppression of intimal hyperplasia of vascular grafts with a distal arteriovenous fistula in a rat model. *J Vasc Surg* 2001; **34**: 701–706.
7. Chancey AL, Brower GL, Peterson JT *et al.* Effects of matrix metallopro-teinase inhibition on ventricular remodeling due to volume overload. *Circulation* 2002; **105**: 1983–1988.
8. Perry GJ, Mori T, Wei CC *et al.* Genetic variation in angiotensin-converting enzyme does not prevent development of cardiac hypertrophy or upregulation of angiotensin II in response to aortocaval fistula. *Circulation* 2001; **103**: 1012–1016.
9. Saiura A, Sata M, Hirata Y *et al.* Circulating smooth muscle progenitor cells contribute to atherosclerosis. *Nat Med* 2001; **7**: 382–383.
10. Han CI, Campbell GR, Campbell JH. Circulating bone marrow cells can contribute to neointimal formation. *J Vasc Res* 2001; **38**: 113–119.
11. Shimizu K, Sugiyama S, Aikawa M *et al.* Host bone-marrow cells are a source of donor intimal smooth- muscle-like cells in murine aortic transplant arteriopathy. *Nat Med* 2001; **7**: 738–741.
12. Hillebrands JL, Klatter FA, van den Hurk BM *et al.* Origin of neointimal endothelium and alpha-actin-positive smooth muscle cells in transplant arteriosclerosis. *J Clin Invest* 2001; **107**: 1411–1422.
13. Li J, Han X, Jiang J *et al.* Vascular smooth muscle cells of recipient origin mediate intimal expansion after aortic allotransplantation in mice. *Am J Pathol* 2001; **158**: 1943–1947.
14. Sata M, Saiura A, Kunisato A *et al.* Hematopoietic stem cells differentiate into vascular cells that participate in the pathogenesis of atherosclerosis. *Nat Med* 2002; **8**: 403–409.
15. Hu Y, Davison F, Ludewig B *et al.* Smooth muscle cells in transplant atherosclerotic lesions are originated from recipients, but not bone marrow progenitor cells. *Circulation* 2002; **106**: 1834–1839.
16. Hu Y, Mayr M, Metzler B *et al.* Both donor and recipient origins of smooth muscle cells in vein graft atherosclerotic lesions. *Circ Res* 2002; **91**: e13–e20.
17. Wagers AJ, Sherwood RI, Christensen JL *et al.* Little evidence for developmental plasticity of adult hematopoietic stem cells. *Science* 2002; **297**: 2256–2259.
18. Castier Y, Brandes RP, Leseche G *et al.* p47phox-dependent NADPH oxidase regulates flow-induced vascular remodeling. *Circ Res* 2005; **97**: 533–540.
19. Lindner V, Fingerle J, Reidy MA. Mouse model of arterial injury. *Circ Res* 1993; **73**: 792–796.
20. Moessler H, Mericskay M, Li Z *et al.* The SM 22 promoter directs tissue-specific expression in arterial but not in venous or visceral smooth muscle cells in transgenic mice. *Development* 1996; **122**: 2415–2425.
21. Xu Q. Mouse models of arteriosclerosis: from arterial injuries to vascular grafts. *Am J Pathol* 2004; **165**: 1–10.
22. Kumar A, Lindner V. Remodeling with neointima formation in the mouse carotid artery after cessation of blood flow. *Arterioscler Thromb Vasc Biol* 1997; **17**: 2238–2244.
23. Mattsson EJ, Kohler TR, Vergel SM *et al.* Increased blood flow induces regression of intimal hyperplasia. *Arterioscler Thromb Vasc Biol* 1997; **17**: 2245–2249.
24. Xu Q. Biomechanical-stress-induced signaling and gene expression in the development of arteriosclerosis. *Trends Cardiovasc Med* 2000; **10**: 35–41.
25. Hu Y, Zhang Z, Torsney E *et al.* Abundant progenitor cells in the adventitia contribute to atherosclerosis of vein grafts in ApoE-deficient mice. *J Clin Invest* 2004; **113**: 1258–1265.
26. Ludewig B, Freigang S, Jaggi M *et al.* Linking immune-mediated arterial inflammation and cholesterol-induced atherosclerosis in a transgenic mouse model. *Proc Natl Acad Sci USA* 2000; **97**: 12752–12757.
27. Xu Q. The Impact of progenitor cells in atherosclerosis. *Nat Clin Pract Cardiovasc Med* 2006; **3**: 94–101.
28. Xu Q, Zhang Z, Davison F *et al.* Circulating progenitor cells regenerate endothelium of vein graft atherosclerosis, which is diminished in ApoE-deficient mice. *Circ Res* 2003; **93**: e76–e86.
29. Zou Y, Dietrich H, Hu Y *et al.* Mouse model of venous bypass graft arteriosclerosis. *Am J Pathol* 1998; **153**: 1301–1310.
30. Dietrich H, Hu Y, Zou Y *et al.* Mouse model of transplant arteriosclerosis: role of intercellular adhesion molecule-1. *Arterioscler Thromb Vasc Biol* 2000; **20**: 343–352.
31. Sanes JR, Rubenstein JL, Nicolas JF. Use of a recombinant retrovirus to study post-implantation cell lineage in mouse embryos. *EMBO J* 1986; **5**: 3133–3142.
32. Hu Y, Baker AH, Zou Y *et al.* Local gene transfer of tissue inhibitor of metalloproteinase-2 influences vein graft remodeling in a mouse model. *Arterioscler Thromb Vasc Biol* 2001; **21**: 1275–1280.